Lagrangian velocity and acceleration auto-correlations in rotating turbulence

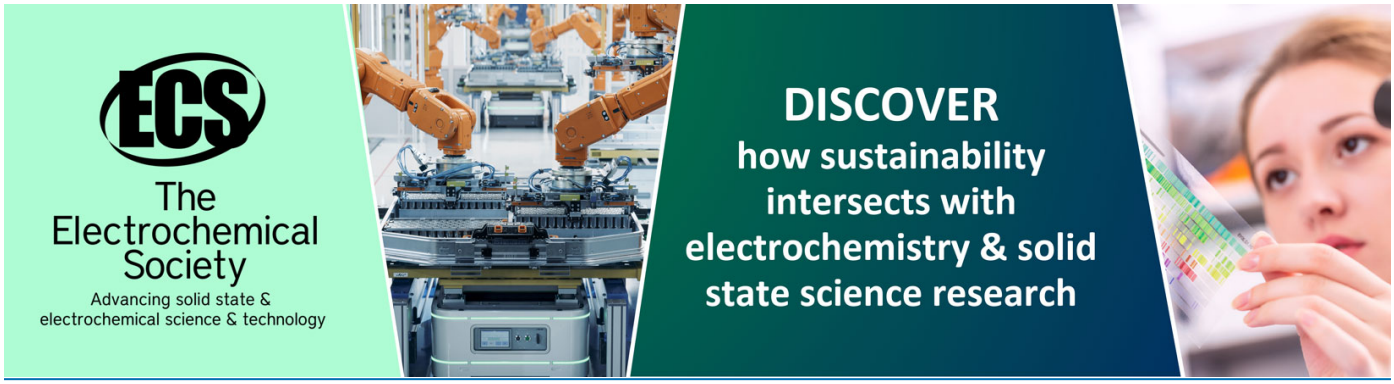

Journal of Physics: Conference Series **318** (2011) 052028 doi:10.1088/1742-6596/318/5/052028

Lagrangian velocity and acceleration auto-correlations in rotating turbulence

L. Del Castello & H.J.H. Clercx

Department of Physics and J.M. Burgers Center for Fluid Dynamics, Eindhoven University of Technology, P.O. Box 513, 5600 MB Eindhoven, The Netherlands

E-mail: h.j.h.clercx@tue.nl

Abstract. Rotating turbulence has often been studied by numerical simulations and analytical models. Experimental data is scarce and purely of Eulerian nature. In the present study, experiments on continuously forced turbulence subjected to background rotation are performed by means of 3D Particle Tracking Velocimetry. The data is processed in the Lagrangian as well as in the Eulerian frame. The background rotation is confirmed to induce two-dimensionalisation of the flow field, and the large-scales are dominated by stable counter-rotating vertical tubes of vorticity. The auto-correlation coefficients along particle trajectories of velocity and acceleration components have been explored. We will discuss the effects of rotation on the Lagrangian temporal scales of the flow.

1. Introduction

The influence of the rotation of the Earth on oceanic and atmospheric currents, as well as the effects of a rapid rotation on the flow inside industrial machineries like mixers, turbines, and compressors, are only the most typical examples of fluid flows affected by rotation. Despite the fact that the Coriolis acceleration term appears in the Navier-Stokes equations with a straightforward transformation of coordinates from the inertial system to the rotating non-inertial one, the physical mechanisms of the Coriolis acceleration are subtle. Several fluid flows affected by rotation have been studied by means of direct numerical simulations and analytical models, see Godeferd & Lollini (1999) and Yeung & Xu (2004). Several experimental studies of rotating turbulence have been carried out (Hopfinger *et al.* (1982); Morize & Moisy (2006); Davidson *et al.* (2006); Van Bokhoven *et al.* (2009); Moisy *et al.* (2011)). However, quantitative experimental data is scarce and purely of Eulerian nature, see Van Bokhoven *et al.* (2009) and Moisy *et al.* (2011). The present work addresses experimentally confined and continuously forced rotating turbulence. In recent experimental investigations on (decaying) rotating turbulence quantitative information is extracted by means of Particle Image Velocimetry (PIV) (Moisy *et al.* (2011)) and stereo-PIV (Van Bokhoven *et al.* (2009)); the present investigation is based on Particle Tracking Velocimetry (PTV), thus acquiring Lagrangian statistics.
A useful insight into the structure of a turbulent flow field is represented by the auto-correlations of the velocity field in the Lagrangian frame. The integral time scales derived from the Lagrangian velocity correlations give a rough estimate of the time a fluid particle remains trapped inside a large-scale eddy, and therefore it might be used as a lower-bound for the typical lifetime of the large eddies. Lagrangian correlations of velocity have been recognised as the key-ingredient

of the process of turbulent diffusion since the work by Taylor (Taylor (1921); Monin & Yaglom (1975)). Since then, the Lagrangian view-point received a growing attention, see the review by Toschi & Bodenschatz (2009). Lagrangian correlations of velocity in nonrotating turbulence were recently measured with an acoustic technique at very high Taylor-based Reynolds number ($Re_\lambda \simeq 800$) and a decay of the correlation coefficients of single velocity components proportional to $e^{-\tau/\tau_0}$ was proposed, with τ_0 comparable to the energy injection time scale, see Mordant *et al.* (2001, 2004a). The same decay has been observed by Gervais *et al.* (2007), who compared Eulerian and Lagrangian correlations of velocity in a $Re_\lambda \simeq 320$ turbulent flow, also relying on acoustic measurements. Here, some of these issues are addressed for rotating turbulence as measured by means of PTV.
The Lagrangian acceleration vector of passive tracers is found to decorrelate with itself on a much shorter time scale than the velocity vector, *i.e.* in a few Kolmogorov times τ_η. In classical Lagrangian models for particle absolute and relative displacement and velocity in turbulent flows, the acceleration correlation was neglected (see table 2 in Pope (1994)). More recent Lagrangian models of turbulent diffusion and mixing treat the particle acceleration in different ways, without neglecting its short but non-vanishing correlation (Jeong & Girimaji (2003); Chevillard & Meneveau (2006)). Yeung (1997) investigated separately the magnitude of the Lagrangian acceleration and its direction from DNS data ($Re_\lambda = 140$), showing that the magnitude remains correlated with itself for much longer time than the very short decorrelation time of the vector direction. Mordant *et al.* (2004b) measured Lagrangian trajectories using high-energy physics particle detectors, which allowed them to retrieve short-time statistics to resolve the highly intermittent Lagrangian acceleration signal at $Re_\lambda \simeq 700$, and to quantify its decorrelation time. A similar experiment, with a more standard high-speed camera system, confirmed these findings, see Xu *et al.* (2007). Statistics of the Lagrangian acceleration (derived from Eulerian measurements) for the highest-Re_λ flow to date were obtained from measurements in the atmospheric boundary layer with a multi-hot-wire probe by Gulitski *et al.* (2007).
In the following Sections we introduce the experimental set-up and procedures, provide a basic flow characterization, present the results for the velocity and acceleration probability distribution functions (PDFs) and autocorrelation functions, and summarize the main conclusions.

2. Experimental set-up

The experimental setup consists of a fluid container, made of transparent perspex in order to ensure optical accessibility, equipped with a turbulence generator, and an optical measurement system. A side view of the set-up is shown in Fig. 1a, and a photograph of the full set-up is shown in Fig. 1b. Four digital cameras (Photron FastcamX-1024PCI) acquire images of the central-bottom region of the flow domain through the top-lid. The fluid is illuminated by means of an LED array composed of 238 Luxeon K2 LEDs (1.4 kW total dissipation and roughly 150 W of light) mounted on a thick aluminium block provided with water-cooling channels. These key elements are mounted on a rotating table, so that the flow is measured in the rotating frame of reference. The inner dimensions of the container define a flow domain of $500 \times 500 \times 250$ mm^3 (length $\times$ width $\times$ height); note that the free surface deformation is inhibited by a perfectly sealed top lid. The turbulence generator is an adaptation of a well-known electromagnetic forcing system commonly used for shallow-flow experiments (see, for example, Sommeria (1986); Tabeling *et al.* (1991); Dolzhanskii *et al.* (1992)), and currently operational in our laboratory for both shallow flow and rotating turbulence experiments (Clercx *et al.* (2003); Akkermans *et al.* (2008); Van Bokhoven *et al.* (2009)). The tank is filled with a highly concentrated sodium chloride (NaCl) solution in water, 28.1% brix (corresponding to 25 g NaCl in 100 g of water). The fluid density ρ_f is 1.19 g/cm^3 and the kinematic viscosity ν is 1.319 mm^2/s. Two titanium elongated electrodes are placed near the bottom at opposite

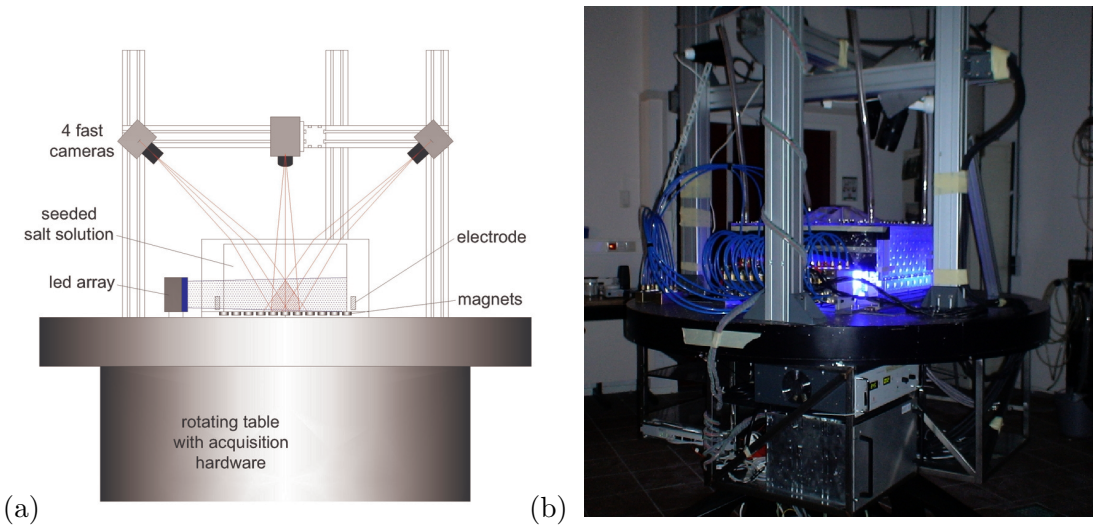

Figure 1. *(a) Schematic drawing of the experimental setup, side view. (b) Photograph of the laboratory set-up.*

sidewalls of the container. A remote-controlled power supply (KEPCO BOP 50 8P) is connected to the electrodes and provides a stable electric current of 8.39 A. An array of axially magnetized permanent (neodymium) magnets is placed directly underneath the bulk fluid. The magnets have a magnetic field strength of approximately 1.4 T at the center of the magnet surface, and they are arranged following a chessboard scheme, *i.e.* alternating North and South poles for the magnets top faces. The magnets, kept in position by a polyvinyl chloride (PVC) frame, are fixed on a 10 mm thick steel plate to increase the density of the magnetic field lines in the fluid bulk. A range of flow scales is forced by using two differently sized magnets, viz., i) elongated bar magnets, $10 \times 10 \times 20$ mm^3 in size; and ii) flat bar magnets, $40 \times 40 \times 20$ mm^3 in size, see Van Bokhoven *et al.* (2009) for more details. With such an arrangement, the largest scales that are forced are comparable with the spacing between adjacent large magnets, i.e., $\mathcal{L}^F = 70$ mm.

The Lagrangian correlations are measured by means of Particle Tracking Velocimetry, making use of the code developed at ETH, Zürich (Maas *et al.* (1993); Malik *et al.* (1993); Willneff (2002); Lüthi *et al.* (2005)). Poly methyl methacrylate (PMMA) particles, with a mean diameter of $d_p = 127 \pm 3 \mu$m and particle density $\rho_p = 1.19$ g/cm^3, are used as flow tracers. The concentration of the salt solution is adjusted to match the PMMA density. The Stokes number (St) for these tracers expresses the ratio between the particle response time and a typical time scale of the flow. For the present experiments it can be estimated as $St = \tau_p/\tau_\eta = \mathcal{O}(10^{-3})$ where $\tau_p = d_p^2/(18\nu)$ is the particle response time (with $\rho_p/\rho_f = 1$) and τ_η is the Kolmogorov time scale of the turbulent flow. The chosen seeding particles can thus be considered as passive flow tracers both in terms of buoyancy and inertial effects. An accurate calibration of the measurement system on a 3D target, followed by the optimization of the calibration parameters on seeded flow images, permits retrieval of the 3D positions of the particles with a maximum error of 9 μm in the horizontal directions and 18 μm in the vertical one. The data are then processed in the Lagrangian frame, where the trajectories are filtered to remove the measurement noise produced by the positioning inaccuracy: Third order polynomials are fitted along limited segments of the trajectories around each particle position. From the coefficients of the polynomial in each point, the 3D time-dependent signals of position and velocity are extracted. With the present setup, up to 2500 particles per time-step have been tracked on average in a volume with size $100 \times 100 \times 100$ mm^3, thus roughly $1.5\mathcal{L}^F$ along each coordinate direction.

A detailed description of the experimental set-up and the data processing routines, together with an in-depth characterization of the flow, can be found in Del Castello (2010).

3. Flow characterisation

The flow is subjected to different background rotation rates $\Omega \in \{0; 0.2; 0.5; 1.0; 2.0; 5.0\}$ rad/s around the vertical z-axis. The measurements are performed when the turbulence is statistically steady (measured by the kinetic energy of the flow). The mean kinetic energy of the turbulent flow is constant in time and decays in space along the upward vertical direction. The flow is fully turbulent in the bottom region of the container where the measurement domain is situated. Eulerian characterisation of the (rotating) turbulent flow with stereo-PIV measurements on horizontal planes has been reported elsewhere (Van Bokhoven *et al.* (2009)). In order to investigate the horizontal homogeneity of the forced flow field in case of no rotation, and to quantify the vertical inhomogeneity, profiles of the rms of the velocity magnitude have been measured in the three directions. The flow appears to be homogeneous to a good approximation in the horizontal directions. On the vertical profile, the corresponding values obtained via stereo PIV measurements (Van Bokhoven *et al.* (2009)) on three horizontal planes yield similar results as our PTV measurements. This agreement is also supported by an almost perfect match between Eulerian horizontal longitudinal integral length scales from stereo PIV and PTV measurements for the range of rotation rates considered, see Del Castello & Clercx (2011). In this investigation it was shown that rotation induces a significant increase of the horizontal length scales up to 1 rad/s and a decrease for faster rotations, in excellent agreement with the stereo PIV measurements. The data by Van Bokhoven *et al.* (2009) also show that the flow is approximately isotropic at midheight in the measurement domain, an important result which can be and is used in the analysis of the present data.
Typical values for the turbulence quantities in our measurement domain are the following. The root-mean-square (rms) velocity averaged over horizontal planes, u_{rms}, is typically in the range of 12 to 18 mm/s. For the Kolmogorov length and time scales we found the typical values 0.6 mm $\lesssim \eta \lesssim$ 0.8 mm and 0.25 s $\lesssim \tau_\eta \lesssim$ 0.55 s, respectively. The Taylor-scale Reynolds number is in the range $70 \lesssim Re_\lambda \lesssim 110$ for all rotation rates. Although the PTV measurements do not provide well-resolved small-scale flow fields, which hampers accurate measurement of the energy dissipation rate, the present data are consistent with those reported by Van Bokhoven *et al.* (2009) (although a milder curent is applied there, 4 A versus 8.39 A for the present set of experiments).

4. Probability distribution functions of velocity and acceleration

The stereo-PIV experiments reveal that the flow is statistically homogeneous in the horizontal plane and approximately statistically isotropic at midheight in the measurement domain. Statistically averaged data from the x- and y-components of the velocity and acceleration vector should yield similar results. We will therefore only consider horizontally averaged PDFs.
We first report on the PDFs of velocity (each one computed on roughly 4×10^6 data points). The PDFs are shown in Fig. 2 in linear-logarithmic scale for all experiments together. Using the assumptions of horizontal homogeneity and isotropy, the PDFs of the x and y component are averaged together and shown in Fig. 2a; in Fig. 2b, the PDF of the z-component is reported. The background rotation is seen to induce only a slight anisotropy of the horizontal components of velocity. The most important effect of rotation is seen on the vertical velocity component, for which the standard deviation of the PDF gets strongly damped for $\Omega = 5.0$ rad/s. The distributions for $\Omega \in \{0; 1.0; 5.0\}$ rad/s are in good quantitative agreement with the ones published by Van Bokhoven *et al.* (2009) (see Figs. 8 and 14 therein). The PDFs have in both cases almost Gaussian shapes (minor skewness) and the kurtosis is only slightly larger

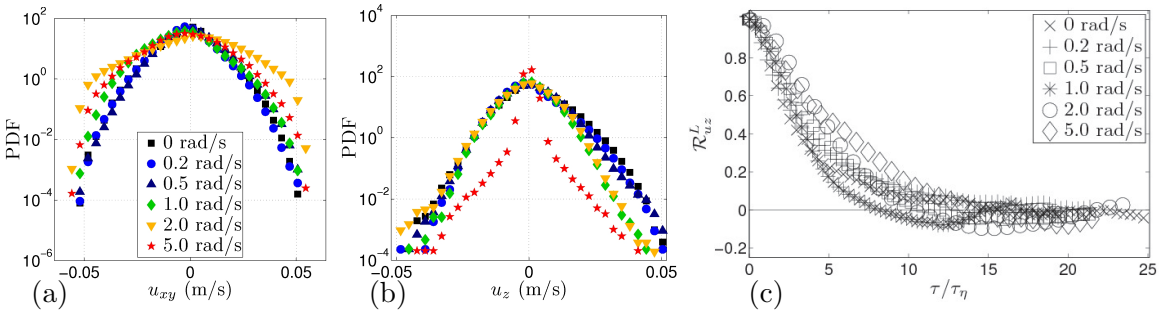

Figure 2. *(a) PDF of the horizontal velocity component $u_h = u_{xy}$ and (b) vertical velocity component u_z for all experiments, in linear-logarithmic scale. (c) Lagrangian auto-correlation coefficients of the Cartesian velocity component u_z for all rotating experiments, with time normalised with τ_η.*

than the Gaussian value. We found $3.0 \lesssim \langle u_i^4\rangle/\langle u_i^2\rangle^2 \lesssim 4.0$, except for the vertical velocity component at $\Omega = 5.0$ rad/s which shows a substantially larger value for the kurtosis. Once more, the latter describes the well-known effect of rotation, which suppresses the fluid motion in the direction of the rotation axis, hence including a strong 2D character of the flow field.

The influence of rotation on the particle acceleration vector is first illustrated with the PDFs, see Fig. 3. The horizontally averaged one (denoted by a_{xy}) is based on roughly 8×10^6 and the z-component on roughly 4×10^6 data points. We compared the PDFs of the acceleration components for the non-rotating experiment with results from the literature (see Voth *et al.* (1998); La Porta *et al.* (2001); Mordant *et al.* (2004b,a); Gulitski *et al.* (2007); Gervais *et al.* (2007)), and observed largely similar features: the distributions are highly non-Gaussian, indicating strong intermittency of the turbulence at the level of accelerations. Due to a slight temporal under-resolution of our measurements, we are not able to measure the highest acceleration events of the turbulence. This is revealed by the end tails of the PDFs, which gets slightly lower for accelerations higher than 0.1 m/s^2. Fortunately, this does not hamper the qualitative comparison of PDFs obtained for different rotation rates, which is the central issue in the current investigation.

Rotation does not influence the PDF of the horizontal acceleration components in a monotonic way. The tails of the PDFs get slightly lower for $\Omega = 0.2$ and 0.5 rad/s. They get higher and significantly higher for $\Omega = 1.0$ and 2.0 rad/s, respectively. Only the end tails get slightly lower when the rotation rate is further increased from 2.0 to 5.0 rad/s. The PDF of the vertical acceleration component, on the contrary, have its tails monotonically lowered as the rotation rate is increased. This indicates the importance of the two-dimensionalisation process induced by rotation which affects the accelerations of passive tracers, despite the same 3D steady forcing is applied to the flow at every rotation rate.

The PDFs shown in Fig. 3 are quantified by extracting values of $\langle a_i^2\rangle$, skewness $S_i = \langle a_i^3\rangle/\langle a_i^2\rangle^{3/2}$ and kurtosis $K_i = \langle a_i^4\rangle/\langle a_i^2\rangle^2$. As can be conjectured from Fig. 3, the PDFs are not appreciably skewed, which is confirmed by the fact that $S_i \approx 0$ for all rotation rates. The values for $\langle a_i^2\rangle$ and K_i (with $i = h$ or z) are presented in Del Castello (2010). Although a slight decrease of $\langle a_i^2\rangle$ is observed for slow rotation ($\Omega \in [0.2; 0.5]$ rad/s), $\langle a_h^2\rangle$ increases substantially for large rotation rates ($\Omega \in [1.0; 5.0]$ rad/s) due to the increase of the horizontal integral length scale with Ω. However, $\langle a_z^2\rangle$ is strongly suppressed. The values for K_h and K_z reveal non-monotonic variations. In fact, a mild background rotation ($\Omega \in [0.2; 0.5]$ rad/s) is seen to amplify the kurtosis of all acceleration components, while a further increase of rotation ($\Omega \in [1.0; 2.0]$ rad/s) induces a reduction of the kurtosis. Such a reduction proceeds when Ω is raised to 5.0 rad/s for what concerns K_h, but K_z, instead, is strongly enhanced for the fastest rotating run, reflecting the strong suppression of a_z induced by rotation. The values for K_i for no or mild

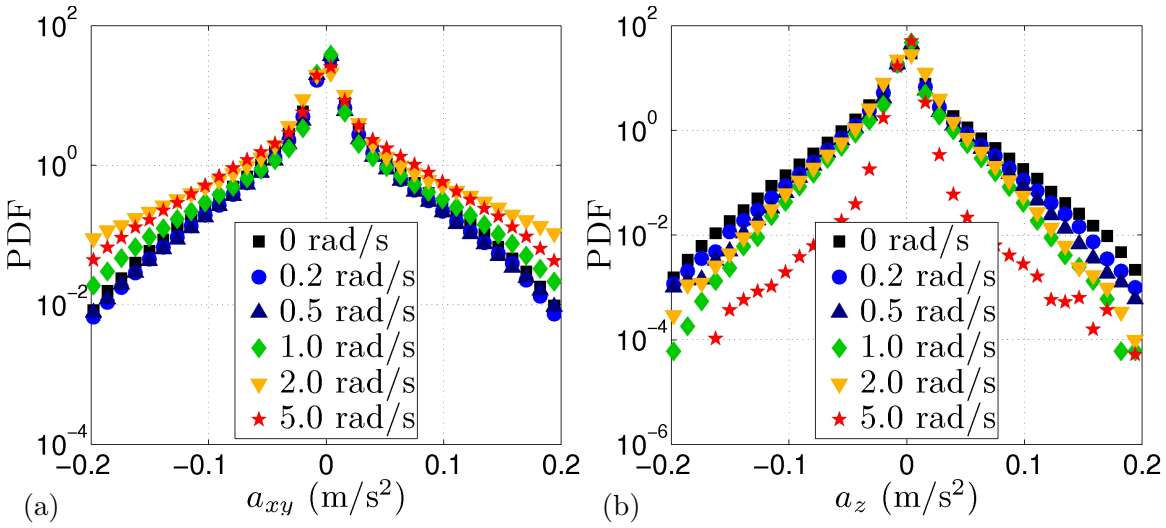

Figure 3. *(color online) PDFs of a_{xy} (a) and a_z (b) of the acceleration for all experiments in linear-logarithmic scale.*

background rotation are also in good agreement with the ones reported in the literature for isotropic turbulence at comparable Re_λ (see, e.g., the inset of Fig. 2(a) in Bec *et al.* (2006)).

5. Lagrangian velocity and acceleration auto-correlations

The auto-correlation coefficients $\mathcal{R}^L_{ui}(\tau)$ for each velocity component $u_i(t)$ (with $i \in 1,2,3$ denoting the x-, y- and z-component, respectively), which are functions of the time separation τ, are obtained averaging over a sufficient number of trajectories, and normalising with the variance of the single component, i.e. $\mathcal{R}^L_{ui}(\tau) \equiv \langle u_i(t)u_i(t+\tau)\rangle / \langle u_i^2(t)\rangle$. As an example, the Lagrangian auto-correlation coefficient of the vertical velocity component u_z is shown in Fig. 2c with time τ normalised with τ_η. The Lagrangian velocity auto-correlations describe clearly a monotonic influence of rotation: the coefficients gets progressively higher for increasing Ω. A stronger Lagrangian auto-correlation is found for the vertical velocity component (relative to those of the horizontal velocity components) than previously reported for the Eulerian temporal velocity correlations, see Van Bokhoven *et al.* (2009).
The Lagrangian acceleration auto-correlation coefficients a_i are obtained similarly: $\mathcal{R}^L_{ai}(\tau) \equiv \langle a_i(t)a_i(t+\tau)\rangle / \langle a_i^2(t)\rangle$. These coefficients decorrelate with itself within several Kolmogorov time scales, and each component shows the well-known negative loop (a mild anti-correlation at short times). The decorrelation process of the Cartesian components is due to the change of the direction of the acceleration vector, rather than to a change of its magnitude. Our measurements of the non-rotating flow confirm the general picture as observed, for example, by Mordant *et al.* (2004a).
We also computed the correlation coefficients of the longitudinal (a_l), the transversal horizontal (a_{th}), and the transversal (partially) vertical (a_{tv}) components of the acceleration vector. This decomposition is sketched in Fig. 4a, where a curved particle trajectory is marked as a thick dotted line, and the transversal plane (the plane perpendicular to the velocity vector $\mathbf{u}$) is denoted as Π_t. The acceleration vector $\mathbf{a}$ is first decomposed into its longitudinal and transversal components, where the longitudinal acceleration is defined as $a_l = \mathbf{a}\cdot\hat{\mathbf{u}}$ (with $\hat{\mathbf{u}} \equiv \mathbf{u}/|\mathbf{u}|$). The transversal horizontal acceleration is defined as the projection over the direction $\mathbf{h}$: $a_{th} = \mathbf{a}\cdot\mathbf{h}$, with $\mathbf{h}\cdot\mathbf{u} = 0$, $\mathbf{h}\cdot\mathbf{e}_z = 0$, and $|\mathbf{h}| = 1$. The transversal (partially) vertical acceleration is defined as the remaining component, $a_{tv} = |\mathbf{a} - a_l\hat{\mathbf{u}} - a_{th}\mathbf{h}|$. The correlation coefficients of the modulus

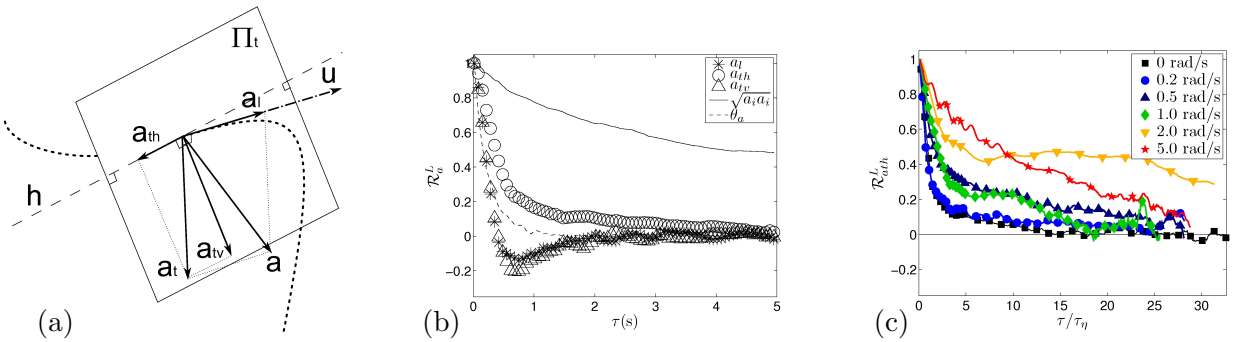

Figure 4. *(a) Sketch of the decomposition of the acceleration in the longitudinal (a_l), transversal (partially) vertical (a_{tv}), and transversal horizontal (a_{th}) acceleration components. (b) Correlations of the acceleration components a_l, a_{tv}, and a_{th}, the modulus of acceleration $|\mathbf{a}|$, and its polar angle θ_a in the horizontal xy-plane. (c) The Lagrangian auto-correlation coefficients of a_{th} for all experiments. The time is normalised with the Kolmogorov time scale τ_η.*

and the polar angle of the acceleration vector, together with the correlation coefficients of a_l, a_{th}, a_{tv}, all for the non-rotating experiment, are shown in Fig. 4b. We are particularly interested in this decomposition because the Coriolis acceleration acts solely in the direction perpendicular to the rotation axis, and perpendicular to the velocity vector.
The Lagrangian auto-correlation coefficients of the Cartesian acceleration components a_i and the components a_l, a_{tv}, and a_{th} have been computed. The effects of rotation on the correlations of the Cartesian components get appreciable for $\Omega = 1.0$ rad/s, and important for $\Omega = 2.0$ and 5.0 rad/s. For these runs, the time scale of the decorrelation process is significantly increased, as revealed by the temporal shift of the negative loop of the correlations of the horizontal components, and to a lesser extent of the vertical component. The correlations of the longitudinal and transversal (partially) vertical components are only mildly affected by rotation, even for the highest rotation rates. The transversal horizontal component of the acceleration vector is instead strongly affected by the background rotation, see Fig.4c. This confirms the direct role played by the Coriolis acceleration in the amplification of the Lagrangian acceleration correlation in rotating turbulence.

6. Conclusions

Comparison of the Lagrangian data for the velocity auto-correlations with Eulerian measurements Van Bokhoven *et al.* (2009) suggests that fluid parcels, being restricted to coherent flow structures, have limited access to vertical velocity variations when the rotation rate is increased. Eulerian measurements would over-estimate the sampling over vertical velocity fluctuations. Rotation suppresses high-acceleration events (reduced intermittency) along the direction parallel to the rotation axis, and amplifies the auto-correlation of the component of the transversal acceleration perpendicular to the rotation axis.

Acknowledgements: This project has been funded by the Netherlands Organisation for Scientific Research (NWO) under the Innovational Research Incentives Scheme grant ESF.6239. The institutes IGP and IfU of ETH (Zürich) are acknowledged for making available the PTV code.

References

Akkermans, R.A.D., Cieslik, A.R., Kamp, L.P.J., Trieling, R.R., Clercx, H.J.H. &

van Heijst, G.J.F. 2008 The three-dimensional structure of an electromagnetically generated dipolar vortex in a shallow fluid layer. *Phys. Fluids* **20**, 116601.

Bec, J., Biferale L., Boffetta, G., Celani, A., Cencini, M., Lanotte, A.S., Musacchio, S. & Toschi, F. 2006 Acceleration statistics of heavy particles in turbulence. *J. Fluid Mech.* **550**, 349.

van Bokhoven, L.J.A., Clercx, H.J.H., van Heijst, G.J.F. & Trieling R.R. 2009 Experiments on rapidly rotating turbulent flows. *Phys. Fluids* **21**, 096601.

Chevillard, L. & Meneveau, C. 2006 Lagrangian dynamics and statistical geometric structure of turbulence. *Phys. Rev. Lett.* **97**, 174501.

Clercx, H.J.H., van Heijst, G.J.F. & Zoeteweij, M.L. 2003 Quasi-two-dimensional turbulence in shallow fluid layers: The role of bottom friction and fluid layer depth. *Phys. Rev. E* **67**, 066303.

Davidson, P.A., Staplehurst, P.J. & Dalziel, S.B. 2006 On the evolution of eddies in a rapidly rotating system. *J. Fluid Mech.* **557**, 135.

Del Castello, L. 2010 *Table-top rotating turbulence: an experimental insight through Particle Tracking*, PhD-thesis Eindhoven University of Technology, The Netherlands.

Del Castello, L. & Clercx, H.J.H. 2011 Lagrangian velocity autocorrelations in statistically steady rotating turbulence. *Phys. Rev. E* **83**, 056316.

Dolzhanskii, F.V., Krymov, V.A. & Manin, D.Y. 1992 An advanced experimental investigation of quasi-two-dimensional shear flows. *J. Fluid Mech.* **241**, 705.

Gervais, P., Baudet, C. & Gagne, Y. 2007 Acoustic Lagrangian velocity measurement in a turbulent air jet. *Exp. Fluids* **42**, 371.

Godeferd, F.S. & Lollini, L. 1999 Direct numerical simulations of turbulence with confinement and rotation. *J. Fluid Mech.* **393**, 257.

Gulitski, G., Kholmyansky, M., Kinzelbach, W., Lüthi, B., Tsinober, A. & Yorish, S. 2007 Velocity and temperature derivatives in high-Reynolds-number turbulent flows in the atmospheric surface layer. Part 1. Facilities, methods and some general results. *J. Fluid Mech.* **589**, 83.

Hopfinger, E.J., Browand, F.K. & Gagne, Y. 1982 Turbulence and waves in a rotating tank. *J. Fluid Mech.* **125**, 505.

Jeong, E. & Girimaji, S.S. 2003 Velocity-gradient dynamics in turbulence: Effect of viscosity and forcing. *Theor. Comput. Fluid Dyn.* **16**, 421.

La Porta, A., Voth, G.A., Crawford, A.M., Alexander, J. & Bodenschatz, E. 2001 Fluid particle accelerations in fully developed turbulence. *Nature* **409**, 1017.

Lüthi, B., Tsinober, A. & Kinzelbach W. 2005 Lagrangian measurement of vorticity dynamics in turbulent flow. *J. Fluid Mech.* **528**, 87.

Maas, H.G., Gruen, A. & Papantoniou, D.A. 1993 Particle tracking velocimetry in three-dimensional flows. Part I: Photogrammetric determination of particle coordinates. *Exp. Fluids* **15**, 133.

Malik, N.A., Dracos, T. & Papantoniou, D.A. 1993 Particle tracking velocimetry in three-dimensional flows. Part II: Particle tracking. *Exp. Fluids* **15**, 279.

Moisy, F., Morize, C., Rabaud, M. & Sommeria, J. 2011 Decay laws, anisotropy and cyclone-anticyclone asymmetry in decaying rotating turbulence. *J. Fluid Mech.* **666**, 5-35.

Monin A.S. & Yaglom A.M. 1975 *Statistical Fluid Mechanics*, MIT Press, Cambridge, MA.

Mordant, N.,Metz, P., Michiel, O. & Pinton, J.-F. 2001 Measurements of Lagrangian Velocity in Fully Developed Turbulence. *Phys. Rev. Lett.* **87**, 214501.

Mordant, N., Leveque, E. & Pinton, J.-F. 2004 Experimental and numerical study of the Lagrangian dynamics of high Reynolds turbulence. *New J. Phys.* **6**, 116.

Mordant, N., Crawford, A.M. & Bodenschatz E. 2004 Three-dimensional structure of the Lagrangian acceleration in turbulent flows. *Phys. Rev. Lett.* **93**, 214501.

Morize, C. & Moisy, F. 2006 Energy decay of rotating turbulence with confinement effects. *Phys. Fluids* **18**, 065107.

Pope, S.B. 1994 Lagrangian PDF methods for turbulent flows. *Annu. Rev. Fluid Mech.* **26**, 23.

Sommeria, J. 1986 Experimental study of the two-dimensional inverse energy cascade in a square box. *J. Fluid Mech.* **170**, 139.

Tabeling, P., Burkhart, S., Cardoso, O. & Willaime, H. 1991 Experimental study of freely decaying two-dimensional turbulence. *Phys. Rev. Lett.* **67**, 3772.

Taylor, G.I. 1921 Diffusion by continuous movements. *Proc. R. Soc. London. Series A* **20**, 196.

Toschi F. & Bodenschatz E. 2009 Lagrangian properties of particles in turbulence. *Annu. Rev. Fluid Mech.* **41**, 375.

Voth G.A., Satyanarayan, K. & Bodenschatz E. 1998 Lagrangian acceleration measurements at large Reynolds numbers. *Phys. Fluids* **10**, 2268.

Willneff, J. 2002 3D particle tracking velocimetry based on image and object space information. *Int. Arch. Photogrammetry and Remote Sensing and Spatial Inform. Sci.* **34**, 601.

Xu, H., Ouellette, N.T., Vincenzi, D. & Bodenschatz, E. 2007 Acceleration Correlations and Pressure Structure Functions in High-Reynolds Number Turbulence. *Phys. Rev. Lett.* **99**, 204501.

Yeung, P.K. 1997 One- and two-particle Lagrangian acceleration correlations in numerically simulated homogeneous turbulence. *Phys. Fluids* **9**, 2981.

Yeung, P.K. & Xu, J. 2004 Effects of rotation on turbulent mixing: Nonpremixed passive scalars. *Phys. Fluids* **16**, 93.